ISA Transactions ■ (■■■■) ■■■–■■■

Contents lists available at ScienceDirect

ISA Transactions

journal homepage: www.elsevier.com/locate/isatrans

Research article

Sliding mode disturbance observer-based control of a twin rotor MIMO system

Ramy Rashad [a], Ayman El-Badawy [b,1,*], Ahmed Aboudonia [a]

[a] Mechatronics Department, Faculty of Engineering and Materials Science, German University in Cairo, Cairo, Egypt
[b] Mechanical Engineering Department, Al-Azhar University and German University in Cairo, Cairo, Egypt

ARTICLE INFO

Article history:
Received 31 August 2015
Received in revised form
12 October 2016
Accepted 13 April 2017

Keywords:
Twin rotor
Sliding mode control
Disturbance observer

ABSTRACT

This work proposes a robust tracking controller for a helicopter laboratory setup known as the twin rotor MIMO system (TRMS) using an integral sliding mode controller. To eliminate the discontinuity in the control signal, the controller is augmented by a sliding mode disturbance observer. The actuator dynamics is handled using a backstepping approach which is applicable due to the continuous chattering-free nature of the command signals generated using the disturbance observer based controller. To avoid the complexity of analytically differentiating the command signals, a first order sliding mode differentiator is used. Stability analysis of the closed loop system and the ultimate boundedness of the tracking error is proved using Lyapunov stability arguments. The proposed controller is validated by several simulation studies and is compared to other schemes in the literature. Experimental results using a hardware-in-the-loop system validate the robustness and effectiveness of the proposed controller.

1. Introduction

Over the past three decades, sliding mode control (SMC) has received significant interest for control system design. The discontinuous nature of the control action is the most distinguished characteristic of SMC that results in very robust control systems which includes complete rejection of disturbances and insensitivity to parametric uncertainties. The main obstacle remaining for sliding mode control to be one of the most useful discoveries in modern control theory is the chattering phenomenon [1]. Therefore, the control research community has focused on developing techniques to solve this challenging problem.

A new concept has been introduced recently which is the sliding mode controller driven by a sliding mode disturbance observer (SMDO-SMC) [2,3]. In this approach, the controller consists of two components; The first one is a conventional continuous feedback term while the second component is responsible for disturbance rejection and is derived from the sliding mode disturbance observer. The main advantage of this approach is that chattering is no longer problematic as it is localized inside a high-frequency loop that bypasses the plant dynamics [1].

In several studies, the backstepping technique and sliding mode control have been combined to develop effective control systems for uncertain nonlinear systems. The authors in [4] have utilized second order sliding modes in a backstepping procedure to compensate disturbances. However, the method is restricted to disturbances dependent only on the states. Authors in [5] proposed a control algorithm based on quasi-continuous higher order sliding modes combined with a backstepping procedure. However, the proposed method is restricted only to systems in strict feedback form. More recently, [6] proposed a controller based on the backstepping procedure and combines the feedback linearization technique with high order sliding modes. The proposed controller handles matched and unmatched disturbances and provides a continuous control signal unlike the previous two studies.

In this study, we address the problem of designing a SMDO based controller for an experimental setup known as the twin rotor multi-input multi-output system (TRMS). The TRMS is a laboratory setup which resembles a helicopter prototype designed for flight control experiments as shown in Fig. 1. The control system design of the TRMS is challenging since its mathematical model is a high order nonlinear system with heavy cross-coupling effects between the two propellers [7]. In the literature, several research studies have been carried out to design control systems for the TRMS test bed. In [8], the TRMS model is decoupled into two single-input single-output (SISO) subsystems and a robust deadbeat controller was designed for each one while the cross couplings were considered as disturbance for each subsystem. In [9], genetic algorithm based proportional derivative and integral

* Corresponding author.
E-mail addresses: ramy.abdelmonem@guc.edu.eg (R. Rashad), ayman.elbadawy@guc.edu.eg (A. El-Badawy), ahmed.abou-donia@guc.edu.eg (A. Aboudonia).
[1] Faculty of Engineering and Material Science German University in Cairo New Cairo City - Al Tagamoa Al Khames, 11835, Egypt.

http://dx.doi.org/10.1016/j.isatra.2017.04.013
0019-0578/

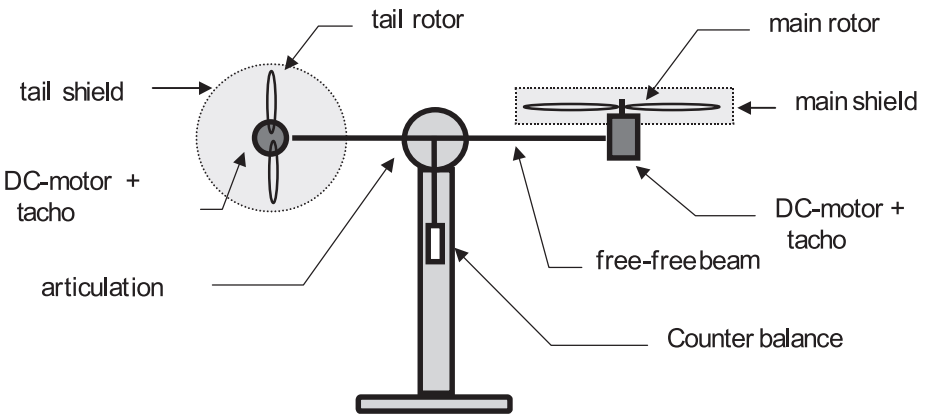

Fig. 1. TRMS Schematic diagram [19].

(PID) control has been utilized for the tracking control of the TRMS. In [10], a decoupled compensator for the TRMS based on a linearized model. The developed controller ensures decoupling in the responses between the horizontal and vertical subsystems. Moreover, in [11] a model predictive control approach is developed for constrained nonlinear systems and the TRMS was used as a test bed to evaluate the validity of the proposed approach. Fuzzy logic control has been used for the design of tracking controllers in several studies as in [12,13] which included also experimental validation of the presented controllers.

On the other hand, SMC has been utilized for the control of the TRMS to increase the robustness of the system to parametric uncertainties and external disturbances. In [14], a second order sliding mode controller was developed and simulated for the TRMS while in [15] the same authors extended their work to include adaptation laws to estimate the unknown bounded system uncertainty. In [7] the authors combined SMC with fuzzy techniques that have been utilized to alleviate the chattering phenomenon present in the conventional SMC.

In the approaches [7,14,15], the authors developed the controllers for a pseudo-decomposed model of the TRMS. In such model the horizontal and vertical subsystems are assumed to be decoupled and the cross couplings between the two subsystems are considered as uncertainties to be handled by the sliding mode controllers developed for linearized models. Although this approach simplifies the control system design, the discontinuity in the control signal's derivative would be required to be larger than the uncertainties upper bound which include the unmodeled nonlinear dynamics in addition to external disturbances. Their approach then computes the actual control signal by integrating its derivative, thus chattering is attenuated.

In this paper, a sliding mode controller driven by a sliding mode disturbance observer is utilized to develop a tracking controller for the TRMS. A nonlinear SMC law is derived and driven by a SMDO which provides estimates of the unmodeled dynamics and external disturbances present in the system. Hence, chattering in the control signals is eliminated rather than attenuated. In addition, the proposed approach can handle arbitrary external disturbances without affecting the continuous nature of the control signals. This is in contrast to the approaches in [7,14,15] which require a higher discontinuity to reject higher disturbances, thus chattering might appear. Moreover, the proposed controller is developed for the nonlinear model instead of the pseudo-decomposed model. The nonlinear model is formulated in a quasi-cascaded structure which allows the actuator dynamics to be handled by a backstepping technique instead of including it in the sliding surface. This multi-step design is favorable due to the natural time scale separation between the actuator dynamics and the remaining dynamics of the TRMS. The backstepping approach is applicable only due to continuous command signals provided by the SMDO based controller. A drawback associated with the backstepping technique is that the time derivatives of the command signals is required. The direct differentiation of these signals would be impractical as real time applications will contain high frequency noise on these signals. Therefore a sliding mode differentiator is utilized to provide estimates of these signal derivatives.

The proposed controller is compared to other approaches combining backstepping and sliding mode techniques as follows: The approaches of [4,5] suffer the disadvantage of discontinuous control action which is remedied in our work using the SMDO. The control approach in [6] consists of the conventional backstepping procedure with the disturbances estimated using a sliding mode observer. The sliding mode observer is used a second time as a differentiator to calculate the command signals derivatives that are required in the normal backstepping process. In our work, we utilized the same sliding mode observer used by [6] but only once for the purpose of differentiating command signals. A disadvantage in the approach of [6] is that the consecutive application of the observer could lead to the deterioration of the closed loop stability, as mentioned in a more recent study by [16].

The proposed controller is implemented in simulation and its effectiveness is tested through several simulation scenarios. These scenarios include tracking pre-specified trajectories and stabilization of the system states in the presence of disturbances due to partial actuator failure. Moreover, the proposed approach is compared in simulation to other control schemes in the literature. Finally, experimental validation of the proposed controller on a laboratory setup through a hardware-in-the-loop system is carried out and the results are presented and discussed.

2. Dynamic model

The TRMS is a laboratory setup designed for flight control experiments as shown in Fig. 1. It is perceived as a static test rig for a helicopter with several control challenges [8]. It consists of two rotors, the main rotor and tail rotor, driven by DC motors and perpendicular to each other. The two rotors are connected by a beam pivoted on its base such that it can rotate in both the vertical and horizontal planes. The motion of the beam is damped by a counterbalance arm with a weight at its end hanging from the central pivot point. The input to the TRMS are the supply voltages of the DC motors which consequently change the speeds of the two rotors and thus the aerodynamic forces generated by the propellers.

The mathematical model of the TRMS has been developed in several studies [17,18]. Throughout this article, the subscripts (h)

Please cite this article as: Rashad R, et al. Sliding mode disturbance observer-based control of a twin rotor MIMO system. ISA Transactions (2017), http://dx.doi.org/10.1016/j.isatra.2017.04.013

and (v) will denote the horizontal and vertical axes respectively. First, the rotors model consists of a linear dynamic system followed by a static nonlinearity [13]. The linear dynamic systems are first order transfer functions given by

$$\frac{u_{hh}(s)}{U_h(s)} = \frac{1}{T_{tr}s+1}, \quad \frac{u_{vv}(s)}{U_v(s)} = \frac{1}{T_{mr}s+1}, \tag{1}$$

where T_{mr}, T_{tr} are the main rotor and tail rotor time constants, U_h, U_v are the supply voltages and u_{hh}, u_{vv} are their filtered counterparts. The two static nonlinear functions which determine the dependance of the DC motor angular velocity on input voltage are given by

$$\omega_h = P_{h1}(u_{hh}), \quad \omega_v = P_{v1}(u_{vv}), \tag{2}$$

while the dependance of the propeller thrust on the motor angular velocity is characterized by two nonlinear functions given by

$$F_h = P_{h2}(\omega_h), \quad F_v = P_{v2}(\omega_v), \tag{3}$$

which are identified experimentally using an electronic balance instead of performing aerodynamic modeling of the rotors [18].

A summary of the mathematical model of the TRMS horizontal and vertical subsystems is given as follows:

$$\begin{aligned}
\dot{H}_h &= F_h l_t \cos(\alpha_v) - f_h \Omega_h \\
\Omega_h &= \frac{H_h + J_{mr}\omega_v \cos(\alpha_v)}{J_h(\alpha_v)} \\
\dot{\alpha}_h &= \Omega_h \\
\dot{H}_v &= F_v l_m - f_v \Omega_v + g[(A-B)\cos(\alpha_v) \\
&\quad -C\sin(\alpha_v)] - \Omega_h^2(A+B+C)\cos(\alpha_v)\sin(\alpha_v) \\
\Omega_v &= \frac{H_v + J_{tr}\omega_h}{J_v} \\
\dot{\alpha}_h &= \Omega_v.
\end{aligned} \tag{4}$$

The parameters in Eq. (4) are defined as follows: α_h, α_v are the yaw and pitch angles of TRMS beam, Ω_h, Ω_v are the yaw and pitch angular rates of the beam, H_h,H_v are the angular momentum in the horizontal and vertical planes of the beam, l_t,l_m are the lengths of the tail part and main part of the beam, $f_h f_v$ are the viscous friction coefficients, J_{tr}, J_{mr} are constant moments of inertia of the tail and main propellers in their axes, $J_h J_v$ are moments of inertia functions in the horizontal and vertical axes, and g denotes the gravitational acceleration. The moment of inertia function J_h is given as $J_h(\alpha_v) = D\sin^2(\alpha_v) + E\cos^2(\alpha_v) + F$. Finally, the terms A, B, C, D, E, F are constants depending on the geometrical and mass properties of the TRMS. The exact expressions of these constants in addition to the detailed derivation of the aforementioned model can be found in [17], while the model parameters provided by the manufacturer can be found in [19].

To obtain a more comprehensible model of the TRMS, the dynamic equations of motion will be rewritten in state space form that do not depend on the angular momentum explicitly. First the state variables are chosen as

$$x_p = \left[\underbrace{\alpha_h, \alpha_v}_{x_1}, \underbrace{\Omega_h, \Omega_v}_{x_2}, \underbrace{u_{hh}, u_{vv}}_{x_3}\right]^\top, \tag{5}$$

while the input vector is given by

$$u_p = [U_h, U_v]^\top. \tag{6}$$

The state equations are then given by

$$\begin{aligned}
\dot{x}_{11} &= x_{21} \\
\dot{x}_{12} &= x_{22} \\
\dot{x}_{21} &= \frac{1}{J_h}\Big[F_h l_t \cos x_{12} - f_h x_{21} - J_{mr}\omega_v x_{22}\sin x_{12} \\
&\quad -x_{21}x_{22}(D-E)\sin(2x_{12}) + \frac{J_{mr}}{T_{mr}}(U_v - x_{32})\frac{dP_{v1}}{dx_{32}}\cos x_{12}\Big] \\
\dot{x}_{22} &= \frac{1}{J_v}\Big[F_v l_m - f_v x_{22} + g\big[(A-B)\cos x_{12} - C\sin x_{12}\big] \\
&\quad -x_{21}^2(A+B+C)\cos x_{12}\sin x_{12} + \frac{J_{tr}}{T_{tr}}(U_h - x_{31})\frac{dP_{h1}}{dx_{31}}\Big] \\
\dot{x}_{31} &= \frac{1}{T_{tr}}(U_h - x_{31}) \\
\dot{x}_{32} &= \frac{1}{T_{mr}}(U_v - x_{32}).
\end{aligned} \tag{7}$$

A detailed derivation of the state space equations can be found in [7].

3. Problem formulation

The control problem considered in this paper is the asymptotic tracking of a reference trajectory $x_1{}^d$ for the yaw and pitch angles of the TRMS. The reference trajectory is assumed to be at least twice differentiable. For the controller design, the state space equations of the TRMS (7) will be rewritten as follows

$$\begin{aligned}
\dot{x}_1 &= x_2 \\
\dot{x}_2 &= f_1(x_1, x_2) + g_1(x_1)\rho_1(x_3) + d \\
\dot{x}_3 &= f_2(x_3) + g_2 u_p,
\end{aligned} \tag{8}$$

where the vectors f_1, f_2 are given by

$$\begin{aligned}
f_1(x_1, x_2) &= [f_{1_h}, f_{1_v}]^\top \\
f_{1_h}(x_1, x_2) &= \frac{1}{J_h}\big[-f_h x_{21} - J_{mr}\omega_v x_{22}\sin x_{12} \\
&\quad -x_{21}x_{22}(D-E)\sin(2x_{12})\big] \\
f_{1_v}(x_1, x_2) &= \frac{1}{J_v}\big[-f_v x_{22} + g((A-B)\cos x_{12} - C\sin x_{12}) \\
&\quad -x_{21}^2(A+B+C)\cos x_{12}\sin x_{12}\big] \\
f_2(x_3) &= \left[-\frac{x_{31}}{T_{tr}}, -\frac{x_{32}}{T_{mr}}\right]^\top,
\end{aligned} \tag{9}$$

while the matrices g_1, g_2 are given by

$$g_1(x_1) = \begin{bmatrix} \frac{l_t \cos x_{12}}{J_h(x_{12})} & 0 \\ 0 & \frac{l_m}{J_v} \end{bmatrix}, \quad g_2 = \begin{bmatrix} \frac{1}{T_{tr}} & 0 \\ 0 & \frac{1}{T_{mr}} \end{bmatrix}. \tag{10}$$

Moreover, using (2)–(3), the vector ρ_1 can be written as

$$\rho_1(x_3) = \begin{bmatrix} F_h \\ F_v \end{bmatrix} = \begin{bmatrix} P_{h2}(\omega_h) \\ P_{v2}(\omega_v) \end{bmatrix} = \begin{bmatrix} P_{h2}(P_{h1}(x_{31})) \\ P_{v2}(P_{v1}(x_{32})) \end{bmatrix}, \tag{11}$$

and finally the disturbance vector d_1 consists of

$$d = \begin{bmatrix} d_1 \\ d_2 \end{bmatrix} = \begin{bmatrix} \frac{1}{J_h}\left[\frac{J_{mr}}{T_{mr}}(U_v - x_{32})\frac{dP_{v1}}{dx_{32}}\cos x_{12}\right] + d_{h,ext} \\ \frac{1}{J_v}\left[\frac{J_{tr}}{T_{tr}}(U_h - x_{31})\frac{dP_{h1}}{dx_{31}}\right] + d_{v,ext} \end{bmatrix}, \tag{12}$$

where $d_{h,ext}$, $d_{v,ext}$ represent unmodeled external disturbances which may occur due to partial actuator failure.

By this formulation it can be observed that the state equations are in a quasi-cascade structure. Thus the approach followed to design the control system is to consider the thrust forces vector ρ_1 as a virtual input to the first two equations in (8). The approach would then to design a SMC law for ρ_1 such that the angles vector x_1 tracks a desired trajectory x_1^d. To reject the disturbance term d, a SMDO is designed to provide an estimate of d which is then used in the control law. The remaining state equations represent the actuator first order dynamics which are assumed to be known as they are of first order and are characterized by the time constants of the actuators. Using the control law for ρ_1, the last step is to design the control laws for the DC motor supply voltages in a backstepping-like approach.

4. Control system design

In this section the SMDO-SMC controller is derived based on Lyapunov stability arguments. The controller is developed for the TRMS dynamics formulated in (8). The design process will be divided into three steps; The first step includes designing an integral SMC for the main system dynamics. The second step consists of designing the SMDO. In the final step, the control law for the motors supply voltages will be designed using the backstepping technique. For analysis purposes, the following assumption is needed

Assumption 1. For $t \geq 0$, the disturbance vector $d(t)$ and its time derivative $\dot{d}(t)$ are continuous and norm bounded, i.e. $\| d(t)\| < F_d$ and $\| \dot{d}(t)\| < \bar{F}_d$ where F_d is a known positive constant and $\bar{F}_d$ is an unknown positive constant.

4.1. Step 1

First we define the tracking error e to be

$$e = x_1^d - x_1, \tag{13}$$

where $x_1{}^d$ represents the desired trajectory for the yaw and pitch angles. Then we define the main sliding variable based on the integral of the tracking error as

$$\sigma = \dot{e} + 2\Lambda e + \Lambda^2 \int_0^t e(\tau)d\tau - \dot{e}(0) - 2\Lambda e(0), \tag{14}$$

where $\Lambda \in \mathbb{R}^{2\times 2}$ is a diagonal positive definite matrix. The choice of the sliding surface in the form (14) makes σ a true measure of tracking performance as it is a filtered version of the tracking error [20]. Moreover, including the last two terms in (14) ensures that the initial value $\sigma(0) \equiv 0$. The advantages of this modification will be discussed later. The controller design proceeds by considering the following virtual subsystem

$$\ddot{x}_1 = \dot{x}_2 = f_1 + g_1\delta_1 + d, \tag{15}$$

where δ_1 is the virtual control input to be designed. Then we choose the following Lyapunov function

$$V_1 = \frac{1}{2}\sigma^\top\sigma, \tag{16}$$

whose time derivative is given by

$$\begin{aligned} \dot{V}_1 &= \sigma^\top\dot{\sigma} \\ &= \sigma^\top\left(\ddot{e} + 2\Lambda\dot{e} + \Lambda^2 e\right) \\ &= \sigma^\top\left(\ddot{x}_1^d + 2\Lambda\dot{e} + \Lambda^2 e - \ddot{x}_1\right) \\ &= \sigma^\top\left(\ddot{x}_1^d + 2\Lambda\dot{e} + \Lambda^2 e - f_1 - g_1\delta_1 - d\right). \end{aligned} \tag{17}$$

4.2. Step 2

Before designing the control input δ_1 we design the SMDO to estimate the bounded disturbance d. The SMDO design begins by defining the auxiliary sliding variable

$$s = \sigma + \xi, \tag{18}$$

where ξ is the SMDO internal variable to be designed. We then consider the following Lyapunov function

$$V_2 = \frac{1}{2}s^\top s, \tag{19}$$

and its time derivative is given by

$$\begin{aligned} \dot{V}_2 &= s^\top\dot{s} = s^\top(\dot{\sigma} + \dot{\xi}) \\ &= s^\top\left(\ddot{x}_1^d + 2\Lambda\dot{e} + \Lambda^2 e - f_1 - g_1\delta_1 - d + \dot{\xi}\right). \end{aligned} \tag{20}$$

By designing the internal variable ξ to have the dynamics given by

$$\dot{\xi} = -\ddot{x}_1^d - 2\Lambda\dot{e} - \Lambda^2 e + f_1 + g_1\delta_1 - \upsilon, \quad \xi(0) = 0, \tag{21}$$

we get

$$\dot{V}_2 = s^\top(-\upsilon - d), \tag{22}$$

where υ is an injection term to be designed. It can be shown easily [21] that the auxiliary sliding variable s is stabilized to zero by means of the classical sliding mode injection term such that

$$\upsilon = K_1 sgn(s), \tag{23}$$

where $K_1 \in \mathbb{R}^{2\times 2}$ is a diagonal positive definite matrix and the function $sgn(\cdot)$ denotes the usual sign function. By this choice of υ we get

$$\begin{aligned} V_2 &= s^\top(-K_1 sgn(s) - d) \\ &\leq -\lambda_{\min}(K_1)\| s \|_1 + F_d \| s \|_1. \end{aligned} \tag{24}$$

By designing the matrix K_1 to have its minimum eigenvalue as $\lambda_{\min}(K_1) = F_d + \eta$, where $\eta > 0$ is a constant, we finally end up with

$$\dot{V}_2 \leq -\eta \| s \|_1, \tag{25}$$

which guarantees the stabilization of s to zero in finite time $t_r \leq \frac{s(0)}{\eta}$ and thus a sliding mode exists in the observer for $t \geq t_r$. By the choice of the sliding surface as in (14), the initial value of the auxiliary sliding variable is $s(0) \equiv 0$, and consequently $t_r \equiv 0$. By the concept of equivalent control [21], the equivalent control term υ_{eq} exactly estimates the negative of the disturbance (d) for $t \geq t_r = 0$. In order to compute an estimate of υ_{eq}, the high frequency switching control action (23) is passed through a low pass filter (LPF), i.e.

$$\hat{\upsilon}_{eq} = \mathrm{LPF}(\upsilon). \tag{26}$$

This indicates that the disturbance d can only be estimated asymptotically with an accuracy proportional to the cut-off frequency of the LPF [22]. The LPF used in this work is a fourth order one with its transfer functions given by

$$\frac{\hat{\upsilon}_{eq,i}(s)}{\upsilon_i(s)} = \frac{1}{(\gamma_i s + 1)^4}, \quad i = 1, 2. \tag{27}$$

The state space implementation of the filters is given by

Please cite this article as: Rashad R, et al. Sliding mode disturbance observer-based control of a twin rotor MIMO system. ISA Transactions (2017), http://dx.doi.org/10.1016/j.isatra.2017.04.013

$$\dot{\omega}_i = \underbrace{\begin{bmatrix} 0 & 1 & 0 & 0 \\ 0 & 0 & 1 & 0 \\ 0 & 0 & 0 & 1 \\ -\frac{1}{\gamma_i^4} & -\frac{4}{\gamma_i^3} & -\frac{6}{\gamma_i^2} & -\frac{4}{\gamma_i} \end{bmatrix}}_{\Gamma_i} \omega_i + \begin{bmatrix} 0 \\ 0 \\ 0 \\ \frac{1}{\gamma_i^4} \end{bmatrix} v_i, \quad i = 1, 2, \tag{28}$$

where $\omega_i = [\omega_{i,1}, \omega_{i,2}, \omega_{i,3}, \omega_{i,4}]^\top$ and $\hat{v}_{eq,i} = \omega_{i,1}$. The selection of the order and cutoff frequency of this filter are selected in practice based on several factors [1]. These factors include the bandwidth of the desired closed loop system and the spectrum of the disturbance. Choosing a very high cut-off frequency for the filter would result in an improved tracking precision, however it is also limited by the actuators bandwidth. Choosing a higher order filter would attenuate high frequency components better but in the same time would cause a larger phase shift in the estimated signal which in return would affect the overall tracking performance. Using the aforementioned guidelines, the filter order and cutoff frequency have been chosen through simulation to achieve the most satisfactory tracking performance.

Now returning to Eq. (17), we can now design the virtual control input δ_1 to be

$$\delta_1 = g_1^{-1}\left(\ddot{x}_1^d + 2\Lambda\dot{e} + \Lambda^2 e - f_1 + \hat{v}_{eq} + K_2\sigma\right), \tag{29}$$

where $K_2 \in \mathbb{R}^{2\times 2}$ is a diagonal positive definite matrix. By assuming that the negative of the disturbance d_1 is exactly estimated by $\hat{v}_{eq}$ we get

$$\dot{V}_1 = -\sigma^\top K_2\sigma < 0, \tag{30}$$

which guarantees that $\sigma \to 0$ as $t \to \infty$ and implies as well that $e, \dot{e} \to 0$ asymptotically. It is worthy to note that the matrix g_1 is non-singular when $-\frac{\pi}{2} < x_{12} < \frac{\pi}{2}$ which is always satisfied based on the physical construction of the TRMS.

4.3. Step 3

The final step of the controller design includes the dynamics of the system actuators given by

$$\dot{x}_3 = f_2 + g_2 u_p. \tag{31}$$

We define the following backstepping variable

$$z = \delta_1 - \rho_1, \tag{32}$$

which corresponds to the difference between the actual and virtual control inputs to the first subsystem (15). By multiplying both sides of (32) by g_1 and substituting (29) we get

$$\begin{aligned} g_1 z &= \underbrace{\ddot{x}_1^d + 2\Lambda\dot{e} + \Lambda^2 e - f_1 - g_1\rho_1 - d}_{\dot{\sigma}} + \hat{v}_{eq} + K_2\sigma + d \\ &= \dot{\sigma} + \hat{v}_{eq} + K_2\sigma + d. \end{aligned} \tag{33}$$

Thus the derivative of the sliding variable σ can be written as

$$\dot{\sigma} = -K_2\sigma + g_1 z - e_d, \tag{34}$$

where $e_d = \hat{v}_{eq} + d \in \mathbb{R}^2$ represents the disturbance estimation error. Then we proceed by choosing the Lyapunov function

$$V_3 = \frac{1}{2}\sigma^\top\sigma + \frac{1}{2}z^\top z. \tag{35}$$

Using (34) and neglecting e_d, the Lyapunov function time derivative can be written as

$$\begin{aligned} \dot{V}_3 &= \sigma^\top\dot{\sigma} + z^\top\dot{z} \\ &= \sigma^\top\left(-K_2\sigma + g_1 z\right) + z^\top\left(\dot{\delta}_1 - \dot{\rho}_1\right) \\ &= -\sigma^\top K_2\sigma + z^\top\left(g_1^\top\sigma + \dot{\delta}_1 - J_1(x_3)\dot{x}_3\right) \\ &= -\sigma^\top K_2\sigma + z^\top\left(g_1^\top\sigma + \dot{\delta}_1 - J_1(x_3)\left(f_2 + g_2 u_p\right)\right), \end{aligned} \tag{36}$$

where J_1 is the *Jacobian* matrix of ρ_1 such as:

$$J_1(x_3) = \frac{\partial\rho_1}{\partial x_3} = \begin{bmatrix} \frac{dF_h}{dx_{31}} & 0 \\ 0 & \frac{dF_v}{dx_{32}} \end{bmatrix}. \tag{37}$$

The stabilization of z can be achieved by designing the control input to be

$$u = g_2^{-1}\left(-f_2 + J_1^{-1}(x_3)\left(\dot{\delta}_1 + g_1^\top\sigma + K_3 z\right)\right), \tag{38}$$

where the existence of g_2^{-1} is guaranteed since g_2 is a constant diagonal matrix as shown in (10). The substitution of the control law (38) in (36) yields

$$\dot{V}_3 = -\sigma^\top K_2\sigma - z^\top K_3 z < 0, \tag{39}$$

which guarantees that $\sigma, z \to 0$ as $t \to \infty$. This concludes the controller design steps where the disturbance estimation error e_d was neglected. In the coming section, the effect of this error on the overall closed loop system will be investigated.

4.4. Closed loop system stability

To analyze the stability of the closed loop system we start by proving the ultimate boundedness of the disturbance estimation error and define the following error vector

$$\begin{aligned} \bar{e} &= [\bar{e}_1^\top, \bar{e}_2^\top]^\top \\ &= [\omega_{1,1} + d_1, \omega_{1,2}, \omega_{1,3}, \omega_{1,4}, \omega_{2,1} + d_2, \omega_{2,2}, \omega_{2,3}, \omega_{2,4}] \end{aligned} \tag{40}$$

where the first and fifth elements of $\bar{e}$ represent the disturbance estimation errors $e_{d,i}$ used in (34) since $\omega_{i,1} = \hat{v}_{eq,i}$. Moreover, the terms d_i are elements of the disturbance vector (12), and $\omega_{i,j}$ represent the states of the low pass filters (28). As discussed previously in Section 4.2, the injection term v exactly estimates the disturbance d by the concept of equivalent control for $t \geq t_r = 0$. Therefore, the error dynamics is given by

$$\dot{\bar{e}}_i = \begin{bmatrix} 0 & 1 & 0 & 0 \\ 0 & 0 & 1 & 0 \\ 0 & 0 & 0 & 1 \\ -\frac{1}{\gamma_i^4} & -\frac{4}{\gamma_i^3} & -\frac{6}{\gamma_i^2} & -\frac{4}{\gamma_i} \end{bmatrix} \bar{e}_i + \begin{bmatrix} 1 \\ 0 \\ 0 \\ 0 \end{bmatrix} \dot{d}_i, \quad i = 1, 2 \tag{41}$$

which can be written in compact form as

$$\dot{\bar{e}} = \underbrace{\begin{bmatrix} \Gamma_1 & 0_{4\times 4} \\ 0_{4\times 4} & \Gamma_2 \end{bmatrix}}_{\Gamma} \bar{e} + g_1(t), \tag{42}$$

where $g_1(t) = [\dot{d}_1(t), 0, 0, 0, \dot{d}_2(t), 0, 0, 0]^\top \in \mathbb{R}^8$, $\Gamma_i \in \mathbb{R}^{4\times 4}$ is defined in (28) and $0_{i\times j}$ represents an $i \times j$ zero matrix.

Due to the choice of $\gamma_i > 0$, it is obvious that Γ_i is a Hurwitz matrix. Thus, by Theorem 4.6 in [23], there exists a unique positive definite symmetric matrix $P \in \mathbb{R}^{8\times 8}$ satisfying

$$P\Gamma + \Gamma^\top P = -I, \tag{43}$$

where $I \in \mathbb{R}^{8\times 8}$ represents the identity matrix. Now we define the following Lyapunov function

$$\bar{V}_1 = \bar{e}^{\top} P \bar{e}, \tag{44}$$

with its time derivative along the trajectories of (42) given by

$$\begin{aligned}\dot{\bar{V}}_1 &= \bar{e}^{\top} P(\Gamma \bar{e} + g_1) + \left(\bar{e}^{\top}\Gamma^{\top} + g_1^{\top}\right) P \bar{e},\\ &= \bar{e}^{\top}(P\Gamma + \Gamma^{\top}P)\bar{e} + 2\bar{e}^{\top} P g_1,\\ &= -\bar{e}^{\top}\bar{e} + 2\bar{e}^{\top} P g_1,\\ &\leq -\| \bar{e} \|^2 + 2\lambda_{max}(P)\bar{F}_d \| \bar{e} \|,\end{aligned} \tag{45}$$

where $\lambda_{max}(P)$ denotes the maximum eigenvalue of the matrix P, $\|\cdot\|$ denotes the *Euclidean* norm, and $\bar{F}_d$ is the upper bound of $\| g_1 \|$ given in Assumption 1. Now we use part of $\| \bar{e} \|^2$ to dominate the positive term in the previous inequality which will be written as

$$\dot{\bar{V}}_1 \leq -(1-\theta)\| \bar{e} \|^2 + 2\lambda_{max}(P)\bar{F}_d \| \bar{e} \| - \theta \| \bar{e} \|^2, \tag{46}$$

where $0 < \theta < 1$. Then,

$$\dot{\bar{V}}_1 \leq -(1-\theta)\| \bar{e} \|^2, \quad \| \bar{e} \| \geq \frac{2\lambda_{max}(P)\bar{F}_d}{\theta}. \tag{47}$$

Thus, by Lemma 9.2 in [23], the solutions of (42) are uniformly ultimately bounded by

$$\| \bar{e}(t)\| \leq \bar{\eta} = \frac{2\lambda_{max}(P)\bar{F}_d}{\theta}\sqrt{\frac{\lambda_{max}(P)}{\lambda_{min}(P)}}, \tag{48}$$

for any initial error $\| \bar{e}(0)\|$. Lemma 9.2 requires that the origin of the unperturbed system with $g_1 \equiv 0$ in (42) to be globally exponentially stable, which is true since Γ is a Hurwitz matrix.

Next we proceed to prove the ultimate boundedness of the tracking error represented by the main sliding variable σ. The closed loop dynamics of the proposed controller is represented by the non-autonomous system

$$\begin{bmatrix}\dot{\sigma}\\ \dot{z}\end{bmatrix} = -\underbrace{\begin{bmatrix}K_2 & 0_{2\times 2}\\ 0_{2\times 2} & K_3\end{bmatrix}}_{K}\begin{bmatrix}\sigma\\ z\end{bmatrix} + \underbrace{\begin{bmatrix}0_{2\times 2} & g_1(t)\\ -g_1^{\top}(t) & 0_{2\times 2}\end{bmatrix}}_{G(t)}\begin{bmatrix}\sigma\\ z\end{bmatrix} + \underbrace{\begin{bmatrix}-e_d(t)\\ 0_{2\times 1}\end{bmatrix}}_{g_2(t)} \tag{49}$$

or equivalently

$$\dot{\varsigma} = -K\varsigma + G(t)\varsigma + g_2(t), \tag{50}$$

which is considered as a non-vanishing perturbation of the nominal system

$$\dot{\varsigma} = -K\varsigma + G(t)\varsigma, \tag{51}$$

with $\varsigma = [\sigma, z]^{\top}$. Since e_d is contained in the error vector $\bar{e}$ (cf. Eq. (40)), the perturbation term satisfies the inequality

$$\| g_2(t)\| = \| e_d(t)\| \leq \| \bar{e}(t)\| \leq \bar{\eta}. \tag{52}$$

Now we prove that the origin $\varsigma = 0$ of the nominal system is exponentially stable. Consider the following Lyapunov function

$$\bar{V}_2 = \frac{1}{2}\varsigma^{\top}\varsigma = \frac{1}{2}\| \varsigma \|^2, \tag{53}$$

with time derivative along the solutions of (51) given by

$$\begin{aligned}\dot{\bar{V}}_2 &= \varsigma^{\top}(-K\varsigma + G\varsigma)\\ &= -\varsigma^{\top}K\varsigma \leq -\lambda_{min}(K)\| \varsigma \|^2 = -2\lambda_{min}(K)\bar{V}_2,\end{aligned} \tag{54}$$

where we used the fact that G is a skew-symmetric matrix such that $\varsigma^{\top}G\varsigma = 0$. Therefore, by Theorem 4.10 in [23], the equilibrium $\varsigma = 0$ is a globally exponentially stable equilibrium point of the nominal system (51). Now we use the Lyapunov function candidate (53) for the perturbed system (50). The derivative of $\bar{V}_2$ along the trajectories of (50) satisfies

$$\begin{aligned}\dot{\bar{V}}_2 &\leq -\lambda_{min}(K)\| \varsigma \|^2 + \| \varsigma \|\| g_2(t)\|\\ &\leq -\lambda_{min}(K)\| \varsigma \|^2 + \bar{\eta} \| \varsigma \|\\ &= -(1-\vartheta)\lambda_{min}(K)\| \varsigma \|^2 - \vartheta\lambda_{min}(K)\| \varsigma \|^2 + \bar{\eta} \| \varsigma \|, \quad 0 < \vartheta < 1\\ &\leq -(1-\vartheta)\lambda_{min}(K)\| \varsigma \|^2, \quad \forall \| \varsigma \| \geq \frac{\bar{\eta}}{\vartheta\lambda_{min}(K)}\end{aligned} \tag{55}$$

Thus, by Lemma 9.2 in [23], the solutions of the perturbed system (50) are uniformly ultimately bounded by

$$\| \varsigma(t)\| \leq \frac{\bar{\eta}}{\vartheta\lambda_{min}(K)}, \tag{56}$$

for any initial state $\| \varsigma(0)\|$, where $\bar{\eta}$ is given by (48). Finally, we conclude that the bounded disturbance estimation error e_d will cause the sliding variable σ to be bounded instead of converge to zero, which leads to tracking within a guaranteed precision rather than perfect tracking [20].

Remark 1. In the design of the control law for the system's input u_p (38), the time derivative of the virtual control input δ_1 is required. However, this derivative can neither be measured nor differentiated directly as it will contain high frequency noise in practice. To overcome such problem, a first order Levant's exact differentiator [24,25] will be used for the estimation of $\dot{\delta}_1$. The sliding mode differentiator will have the form

$$\begin{aligned}\dot{\hat{\delta}}_1 &= -\mu_1\left|\hat{\delta}_1 - \delta_1\right|^{\frac{1}{2}} sgn\left(\hat{\delta}_1 - \delta_1\right) + \bar{\omega}\\ \dot{\bar{\omega}} &= -\mu_2 sgn\left(\hat{\delta}_1 - \delta_1\right),\end{aligned} \tag{57}$$

where μ_1, μ_2 are the design parameters which are chosen to satisfy certain conditions described in [25]. Contrary to the conventional differentiator, a sliding mode differentiator possesses two important properties which are exact differentiation achieved with finite transient time in addition to robustness to any small noise available in the input signal δ_1 [25]. The main contributor of noise in this signal is the discontinuous control action (23). However, this high frequency noise is attenuated through the low pass filter (26). Thus, the noise amplitude in the signal δ_1 is significantly reduced which is then differentiated using (57).

5. Simulation results

The TRMS mathematical model (4) is used to build a MATLAB/Simulink® model to validate the proposed SMDO-SMC approach and test its performance in the presence of disturbances. These disturbances applied to the system include the unmodeled dynamics (12) and external disturbances that may occur due to partial actuator failure. The results of three simulation scenarios will be presented in this section. The first scenario includes tracking a square wave having a frequency of 0.025 Hz and an amplitude of 0.5 and 0.2 rad for the yaw and pitch angles respectively. The second simulation scenario includes tracking a sinusoidal trajectory with the same frequency and amplitudes used in the first scenario. In these cases the initial condition of the TRMS is chosen as $x(0) = [0, -0.5, 0, 0, 0, 0]^{\top}$. A third scenario is simulated to assess the robustness of the proposed approach to external disturbances via the stabilization of the yaw and pitch angles to zero from $x(0) = [0.5, -0.5, 0, 0, 0, 0]^{\top}$. In the middle of the scenario a 50% loss of effectiveness (LoE) in the main rotor's thrust is simulated to resemble a partial actuator failure which may occur due to the propeller damage. The actuator LoE is simulated by multiplying the thrust force generated by the main rotor F_v by a scaling factor.

Please cite this article as: Rashad R, et al. Sliding mode disturbance observer-based control of a twin rotor MIMO system. ISA Transactions (2017), http://dx.doi.org/10.1016/j.isatra.2017.04.013

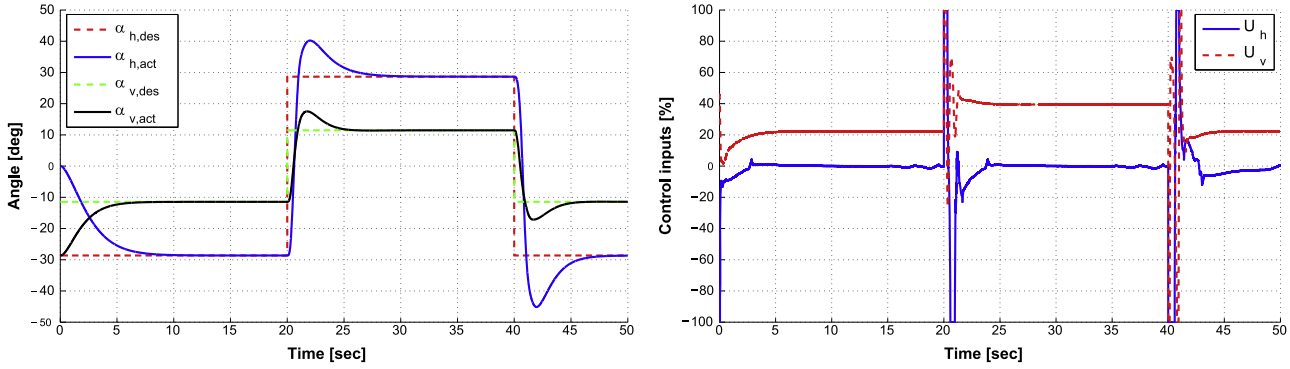

(a) Yaw and pitch angles (b) Control inputs

Fig. 2. Simulation scenario 1: Square wave response of the TRMS using the proposed controller. (a) Yaw and pitch angles. (b) Control inputs.

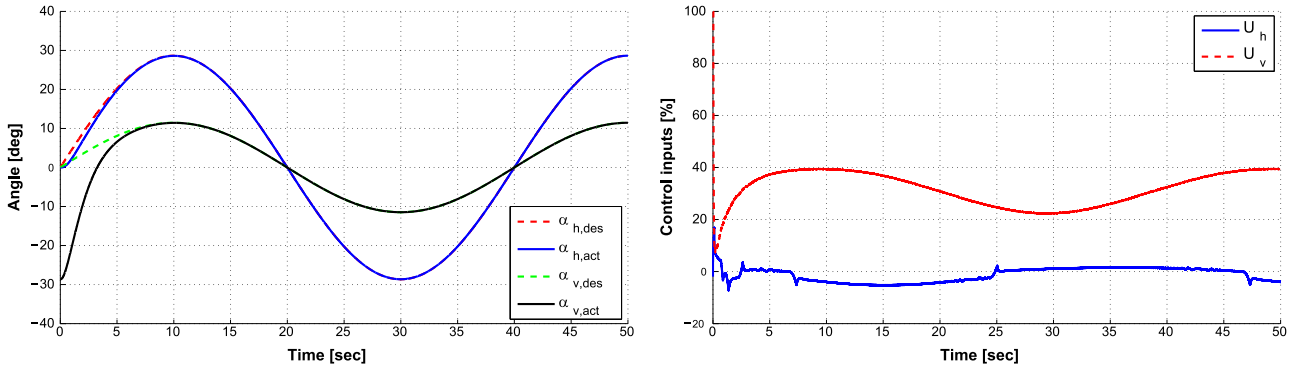

(a) Yaw and pitch angles (b) Control inputs

Fig. 3. Simulation scenario 2: Sine wave response of the TRMS using the proposed controller. (a) Yaw and pitch angles. (b) Control inputs.

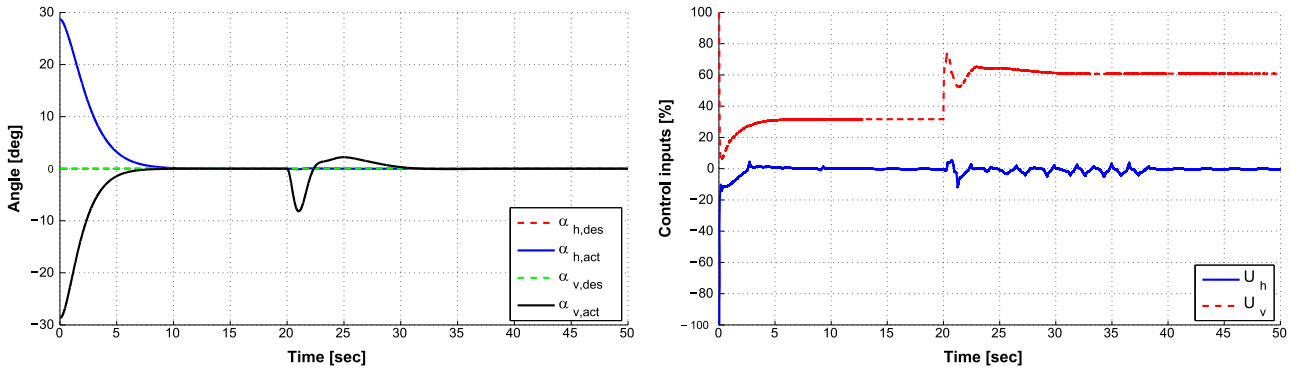

(a) Yaw and pitch angles (b) Control inputs

Fig. 4. Simulation scenario 3: Stabilization of the TRMS using the proposed controller subjected to actuator failure. (a) Yaw and pitch angles. (b) Control inputs.

The simulation results for the three scenarios in Figs. 2–4. It is worthy to mention that all the control signals plots show the pulse width modulation duty cycle percentage of the DC motors which can rotate either clockwise or counter-clockwise. For the first scenario, the desired and actual responses of the TRMS are plotted in Fig. 2a with the control inputs for the main and tail rotor plotted in Fig. 2b. The second scenario, as mentioned before, includes tracking a sinusoidal trajectory shown in Fig. 3a for the yaw and pitch angles respectively. The figures show that a very satisfactory tracking performance was achieved for both the yaw and pitch angles. Finally the control signals generated for the main and tail rotor can be found in Fig. 3b which show a periodic behavior after some transients due to the initial zero velocity of the beam. As for the third scenario, the yaw and pitch angles have successfully converged to zero starting from 0.5 and -0.5 rad ($\approx 30°$) respectively as shown in Fig. 4a. It can also be observed that the pitch angle recovered successfully in the presence of the severe 50% LoE introduced in the simulation at t=20 s. This performance has been achieved using the control action shown in Fig. 4b.

To study the relative performance of the proposed SMDO-SMC approach with other works in the literature, we will compute error and control indices defined to be the sum of their absolute values [15]. This performance criteria was applied by Mondal and Mahanta [15] to compare an adaptive second order sliding mode controller to modified PID controllers by Juang et al. [9]. The PID controllers compared in [9] include conventional PID control, conventional real-value-type genetic algorithm (C-RGA), and modified real-value-type genetic algorithm (M-RGA). All of the

Please cite this article as: Rashad R, et al. Sliding mode disturbance observer-based control of a twin rotor MIMO system. ISA Transactions (2017), http://dx.doi.org/10.1016/j.isatra.2017.04.013

Table 1
Comparison of error indices for different controllers.

Reference	Axis	PID [9]	C-RGA [9]	M-RGA [9]	ASOSM [15]	SMDO-SMC
Square	H	150.22	141.52	134.03	83.70	**80.6**
	V	112.85	96.36	90.21	45.80	**30.76**
Sine	H	23.21	19.33	20.92	32.33	**2.88**
	V	65.74	51.78	52.61	42.20	**22.01**

Table 2
Comparison of control indices for different controllers.

Reference	Axis	PID [9]	C-RGA [9]	M-RGA [9]	ASOSM [15]	SMDO-SMC
Square	H	202	171.28	165.32	**42.34**	57.48
	V	656.37	591.65	551.59	487.29	**299.8**
Sine	H	27.41	20.12	18.93	**10.68**	23.97
	V	611.70	500.2	501.78	515.42	**318.7**

Fig. 5. Experimental setup.

aforementioned control schemes were compared using the same performance criteria mentioned above for the first two scenarios. The error and control indices are calculated from t=0-50 s with a sampling period of 0.05 s and are tabulated in Tables 1 and 2. It is evident from these tables that the proposed SMDO-SMC approach requires less control action to achieve lesser error in a majority of the cases when compared with the other control schemes.

6. Experimental validation

The SMDO-SMC controller was implemented in hardware on the TRMS system shown in Fig. 5. In this system, we implemented the controller in real time using MATLAB/Simulink® in a PC computer. The control and data acquisition is performed using the equipped FPGA (Field Programmable Gate Array) devices which operate in the Xilinx® technology. Two scenarios were conducted for the experiments. The first scenario includes tracking a sinusoidal trajectory for the yaw and pitch angles with twice the frequency used before in the simulation scenarios and amplitudes of 90° and 20° (≈1.57 and 0.35 rad) respectively. As for the second scenario it includes the stabilization of the yaw and pitch angles to zero starting from their equilibrium position. Due to the difficulty of implementing the partial actuator failure for the TRMS propellers in the lab, a constant load is attached to the pitch axis in the middle of the scenario instead. The experimental results of the two scenarios are presented in Figs. 6–7. A common observation in all figures is that the signals are plotted after a small delay of 1 second, which is normal due to the operation of the setup's FPGA devices. The video attached with this article shows the two experiments conducted to verify the proposed control approach.

For the first scenario, Fig. 6a shows that a very satisfactory tracking performance was achieved for the yaw and pitch angles. However, it is observed that the pitch angle performance was not as smooth as the yaw angle. The reason for such performance is the regular disturbance applied on the vertical axis due to gravitational effects which does not affect the horizontal axis. Moreover, some significant deviations can be clearly observed in the time intervals $t = 15 - 20$ s and $t = 35 - 40$ s. The justification of this behavior is that the main rotor is subjected to ground effect disturbances from the supporting base during these intervals which can be seen in the video attached. The control signals generated for the main and tail rotors are presented in Fig. 6b. As for the second scenario, Fig. 7a shows that the yaw and pitch angles successfully converged to zero both from their initial equilibrium and after the constant load is added to the pitch axis. Finally, Fig. 6b shows the control signals for the tail and main DC motors.

7. Conclusion

In this paper, a SMDO-SMC controller is proposed for the tracking control of a TRMS laboratory setup. The proposed

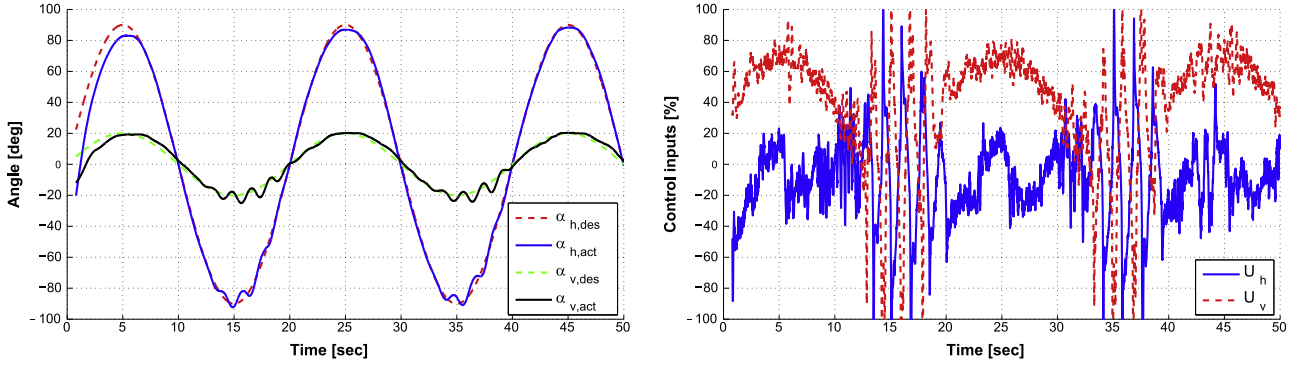

(a) Yaw and pitch angles (b) Control inputs

Fig. 6. Experiment 1: Sine wave response of the TRMS using the proposed controller subjected to ground effect disturbances. (a) Yaw and pitch angles. (b) Control inputs.

Please cite this article as: Rashad R, et al. Sliding mode disturbance observer-based control of a twin rotor MIMO system. ISA Transactions (2017), http://dx.doi.org/10.1016/j.isatra.2017.04.013

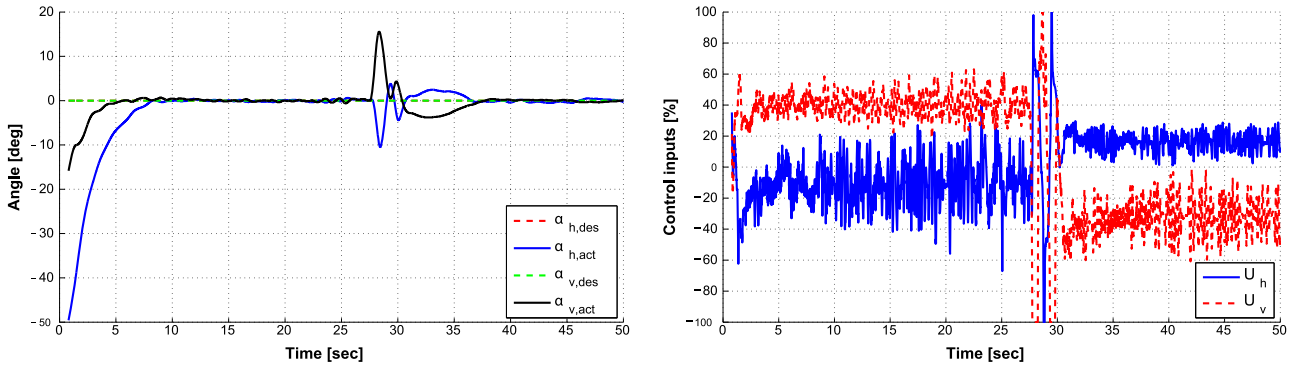

(a) Yaw and pitch angles (b) Control inputs

Fig. 7. Experiment 2: Stabilization of the TRMS using the proposed controller subjected to external disturbance. (a) Yaw and pitch angles. (b) Control inputs.

approach is utilized to provide robustness to unmodeled dynamics and external disturbances including partial actuator failure while preserving the continuity of the supply voltages of the DC motors. In order to validate the proposed controller, the dynamic model of the TRMS is used to build a simulation environment. The simulation studies performed showed that the controller was able to stabilize the tracking errors of the yaw and pitch angles to zero even in the presence of external disturbances and the unmodeled dynamics intentionally left out. A comparison with other control schemes in the literature shows that, in general, the proposed approach can provide less tracking error with lower control effort. Moreover, the proposed controller was implemented in hardware on a TRMS setup and the experimental results were very similar to the simulation results which proves the robustness of the controller to parametric uncertainty, and in the same time proves the validity of the TRMS mathematical model.

Appendix A. Supplementary data

Supplementary data associated with this article can be found in the online version at http://dx.doi.org/10.1016/j.isatra.2017.04.013.

References

[1] Young KD, Utkin VI, Ozguner U. A control engineer's guide to sliding mode control. IEEE Trans Control Syst Technol 1999;7(3):328–42.
[2] Young K, Drakunov S. Discontinuous frequency shaping compensation for uncertain dynamic systems. In: Proceedings of the 12th IFAC World Congress; 1993. p. 39–42.
[3] Hall CE, Shtessel YB. Sliding mode disturbance observer-based control for a reusable launch vehicle. J Guid Control Dyn 2006;29(6):1315–28.
[4] Ferrara A, Giacomini L. On modular backstepping design with second order sliding modes. Automatica 2001;37(1):129–35.
[5] Estrada A, Fridman L. Quasi-continuous HOSM control for systems with unmatched perturbations. Automatica 2010;46(11):1916–9.
[6] Davila J. Exact tracking using backstepping control design and high-order sliding modes. IEEE Trans Autom Control 2013;58(8):2077–81.
[7] Tao C-W, Taur J-S, Chang Y-H, Chang C-W. A novel fuzzy-sliding and fuzzy-integral-sliding controller for the twin-rotor multi-input-multi-output system. IEEE Trans Fuzzy Syst 2010;18(5):893–905.
[8] Wen P, Lu T-W. Decoupling control of a twin rotor MIMO system using robust deadbeat control technique. IET Control Theory A 2008;2(11):999–1007.
[9] Juang J-G, Huang M-T, Liu W-K. PID control using presearched genetic algorithms for a MIMO system. IEEE Trans Syst Man Cybern C Appl Rev 2008;38(5):716–27.
[10] Pradhan JK, Ghosh A. Design and implementation of decoupled compensation for a twin rotor multiple-input and multiple-output system. IET Control Theory A 2013;7(2):282–9.
[11] Rahideh A, Shaheed MH. Stable model predictive control for a nonlinear system. J Frankl Inst 2011;348(8):1982–2004.
[12] Tao C-W, Taur J-S, Chen Y. Design of a parallel distributed fuzzy LQR controller for the twin rotor multi-input multi-output system. Fuzzy Set Syst 2010;161(15):2081–103.
[13] Juang J-G, Liu W-K, Lin R-W. A hybrid intelligent controller for a twin rotor MIMO system and its hardware implementation. ISA Trans 2011;50(4):609–19.
[14] Mondal S, Mahanta C. Second order sliding mode controller for twin rotor MIMO system. In: Proceedings of the Annual IEEE India Conference. IEEE; 2011, p. 1–5.
[15] Mondal S, Mahanta C. Adaptive second-order sliding mode controller for a twin rotor multi-input-multi-output system. IET Control Theory A 2012;6(14):2157–67.
[16] Ferreira de Loza A, Punta E, Fridman L, Bartolini G, Delprat S. Nested backward compensation of unmatched perturbations via HOSM observation. J Frankl Inst 2014;351(5):2397–410.
[17] Chalupa P, Přikryl J, Novák J. Modelling of twin rotor MIMO system. Procedia Eng 2015;100:249–58.
[18] Feedback corporation, twin rotor MIMO system 33-220 user manual; 1998.
[19] Inteco corporation, two rotor aerodynamical system user manual, Available at ⟨http://www.inteco.com.pl⟩, Krakow, Poland; 2011.
[20] Slotine J-JE, Li W, et al. Applied nonlinear control.Englewood Cliffs, NJ: Prentice-hall; 1991.
[21] Shtessel Y, Edwards C, Fridman L, Levant A. Sliding mode control and observation. Springer; 2014.
[22] Li S, Yang J, Chen W-H, Chen X. Disturbance observer based control: methods and applications. CRC Press; 2014.
[23] Khalil HK. Nonlinear systems. 3rd Edition. Prentice hall; 2002.
[24] Levant A. Higher-order sliding modes, differentiation and output-feedback control. Int J Control 2003;76(9–10):924–41.
[25] Levant A. Robust exact differentiation via sliding mode technique. Automatica 1998;34(3):379–84.

Please cite this article as: Rashad R, et al. Sliding mode disturbance observer-based control of a twin rotor MIMO system. ISA Transactions (2017), http://dx.doi.org/10.1016/j.isatra.2017.04.013